Book Chapter

Functionally Graded Materials (FGM) Fabricated by Direct Laser Deposition: A Review

Ferreira AA[1,2]*, Romio PC[1], Sousa JP[2], Omid E[2], Cruz J[3], Reis AR[1,2] and Vieira MF[1,2]*

[1]Faculty of Engineering of the University of Porto, Portugal
[2]LAETA/INEGI—Institute of Science and Innovation in Mechanical and Industrial Engineering, Portugal
[3]SERMEC-Group, Portugal

***Corresponding Authors:** Ferreira AA, Faculty of Engineering of the University of Porto, 4200-465 Porto, Portugal

Vieira MF, Faculty of Engineering of the University of Porto, 4200-465 Porto, Portugal

Published **August 11, 2021**

How to cite this book chapter: Ferreira AA, Romio PC, Sousa JP, Omid E, Cruz J, Reis AR, Vieira MF. Functionally Graded Materials (FGM) Fabricated by Direct Laser Deposition: A Review. In: M Iqbal Khan, editor. Prime Archives in Material Science: 3rd Edition. Hyderabad, India: Vide Leaf. 2021.

Abstract

This review article analyses recent advances in developing functionally graded materials (FGM) produced by Direct Laser Deposition (DLD). Industrial development has supported the

production of new materials that are more efficient and effective, including this new class of composite materials. Initially conceived for the aerospace and nuclear sectors, their application has been extended to several other industrial sectors, such as automotive, biomedical, energy, and military. In addition, FGM manufacturing technologies have evolved from manufacturing conceptual prototypes to creating full-scale end-use components. This article discusses the principal mechanical and metallurgical characteristics of an FGM, the manufacturing processes, with an emphasis on Direct Laser Deposition, material selection, and associated defects. The main challenges in the production of gradient materials are also addressed.

Keywords

Additive Manufacturing; Functionally Graded Materials; Direct Laser Deposition; Microstructure; Mechanical Characterisation

Introduction

Functionally graded materials (FGMs) are characterised by presenting a gradual change in, density, composition, or microstructure from one side to another. This combination is associated with a gradient of properties, either mechanical, thermal, magnetic, chemical, or electrical. FGMs are considered advanced materials that can have excellent properties, not attainable by the materials used alone. With FGMs it is possible to tailor the microstructures/properties leading to the desired performance [1,2]. This non-uniform set of properties across the whole part makes it attractive for a wide range of applications. Aerospace industry use FGMs for rocket components capable of withstanding high loads, presenting a high thermal dissipation capability [3-5]. The automotive industry resources these materials to promote surface wear resistance in engine cylinders [6,7]. Biomedical applications are also a point of interest for FGM materials through the porosity grading of parts, allowing bone or tissue generation [8]. Overall, properties such as corrosion, wear, and oxidation resistance can be added to materials in which properties such as mechanical strength and toughness would prevail [9].

FGM was initially developed for thermal barrier applications by the Japanese space project [10]. It was intended that the material would be able to withstand a gradient of 2000K to 1000K through a 10 mm thickness section. The development of a gradient material was propelled by the constant crack failure of traditional laminate composite materials due to improper interfacial adhesion between materials. The solution for this problem was reducing sharp interfaces by decreasing the particle size and gradually adding the second material, minimizing high-stress concentration points and consequently the failure of the material [7].

FGM can be divided into distinct categories. The joining of different materials, from now on named multi-material FGM, consists in one hand on the fabrication of a part with a mixture of two or more materials, benefiting from their performance result. Also, graded parts can be created in the multi-material category by adding distinct materials in separate layers. The other category is referred to the single material graded parts. Post-processing is applied, getting its microstructural behaviour modified locally (usually at surface level) to promote distinct surface properties [11].

The development of additive manufacturing has expanded the possibilities in the production of these materials, namely allowing FGMs with density gradient [12]. FGMs processing methods are traditionally divided into two groups that depend on the cross-section of material to be produced: thin films and bulk graded materials. Thin films or coatings are produced by methods such as physical vapor deposition (PVD) and chemical vapor deposition (CVD), which are the most common to introduce a gradient of properties without significantly altering the part geometry. These methods are often used to improve mechanical properties at the surface level, distinguishing them from the interior ones. Powder metallurgy and casting fabrication methods such as centrifugal casting, slip casting, and tape casting, unlike coatings, allow the part to be created with a full gradient of properties throughout its entire thickness. Additive manufacturing, specifically Direct Laser Deposition (DLD) technology, brings the opportunity of an alternative and

flexible process, enabling the production and repair of components with this type of functionality, either in bulk, through the deposition of several layers, or on the surface, depositing few layers [2,6].

DLD is an additive manufacturing (AM) technique capable of creating near net shape parts from powder or wire, melting them into the desired geometry, ensuring excellent bonding and metallurgical properties [13-16]. Due to its geometric freedom, scalability, and adaptability to distinct scenarios, that other metal AM technologies cannot offer, DLD is often used for the production of complex and custom parts, and coating/repairing of metal components [17-19]. Yet, the greatest advantage of this technology is the possibility of processing several materials in the same operation, granted with the use of several powder feeders. Therefore, this technology can be assumed to be a multi-material/graded deposition method, as it can simultaneously take advantage of using different powders enabling the deposition of distinct materials in consequent layers or the combination of different amounts of each material in each layer. The DLD equipment, an example of which is shown in Figure 1, is versatile and modular, allowing the manufacture of components with different geometries, including structures with functional gradients, as already mentioned, by a single process, without the use of additional equipment [20].

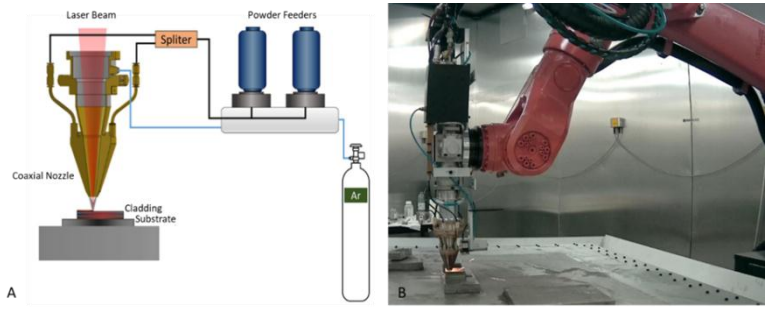

Figure 1: Direct laser deposition (DLD) equipment. (a) Schematic representation of a coaxial configuration with two powder feeders and (b) equipment during processing.

Recently, several works have reviewed the knowledge about the production of FGMs by different AM technologies [7,12,17,21]. In this study, an in-depth analysis is made only on the FGMs produced by DLD, the metallurgical and mechanical properties obtained, and the phenomena involved. This review intends to describe the different approaches adopted, categorizing, and comparing the various advances achieved in the process.

This review is organized into five sections. After the introductory section, there is a section that addresses the state of the art and classification of FGM studies produced with DLD. The description of phenomena involved in the solidification process and the microstructures formed are summarized in the following section. The most common defects in FGMs are described in session four. Finally, the mechanical properties of the FGMs fabricated by DLD are given in the last section.

Production and Characteristics of FGMS

The production of FGM by AM has been the object of study by several research groups [22–24]. From these studies it is evident that production is generally limited to small samples. Extending the construction to larger components with functional gradient properties depends on optimizing the process parameters. These are fundamental for controlling microstructure and improving properties. High-performance and versatile FGMs can meet performance requirements and be used successfully in a variety of industries [3,25].

The ability to mix two or more types of powders and control the feed rate of each flow makes DLD a flexible process for manufacturing complex components, for the innovative development of alloys, and to produce materials with a gradient of functionality [7,22,26]. DLD uses a deposition system equipped with two or more powder feeders that make it possible to create gradients that are traditionally difficult to achieve. This technology makes it possible to produce materials with a gradient at the microstructure level; this gradient is achieved due to localized melting and strong mixing movement in the melt.

Thus, materials can be tailored for functional performance in particular applications.

Using DLD, it is possible to gradually change the composition of a component by controlling the powder feed rate, as shown in Figure 2. The production of these multi-materials improves the interfacial bond between dissimilar materials, minimising chemical and metallurgical incompatibility through the formation of smooth gradients, avoiding the formation of common defects such as porosities and cracks [27,28]. In addition, FGM promotes a better homogenization of the thermal expansion coefficients of two or more different metallic alloys and even other types of material, such as ceramics, where the direct union could lead to the failure of the deposit.

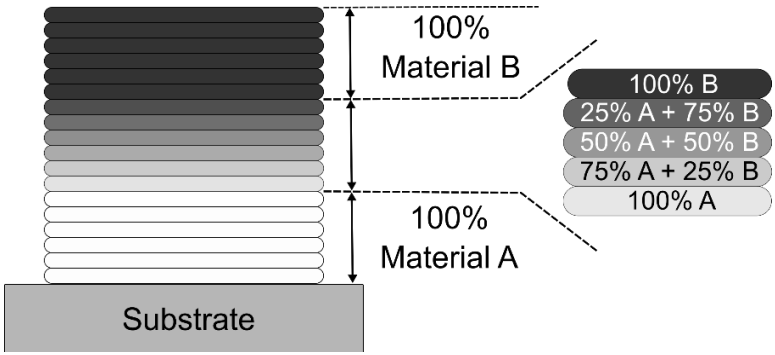

Figure 2: A layered deposition scheme with chemical composition gradient for fabricating an FGM. Adapted from [23].

One of the main factors for producing FGMs by DLD is the proper selection of the mixing of powders that must be in accordance with the metallurgical, mechanical, chemical, and tribological requirements of the components, which is an aspect that promotes innovation [29]. Powders present different densities, and the lighter and smaller particles are carried by the gas flow more easily than the heavy and larger ones, promoting an uneven distribution in particle gradient, thus reducing the performance of the component. The control of the particle size, finding the optimum mixing condition, promotes the

manufacture of gradient materials with great control of the chemical composition and microstructure [30,31].

As the composition of the material varies throughout the FGM, several phases with different chemical compositions will form. These phases help to achieve the intended performance of the FGM for the selected application. The different phases formed depend on the composition of the materials (powders and substrate) and the manufacturing conditions, such as laser power, feed rate, scanning speed, cooling rate, and treatments conducted on the material, emphasizing preheating.

Traditionally, the manufacturing process of an FGM can be divided into two stages: gradation, which consists of building a spatially non-homogeneous structure, and consolidation, which is the transformation of this structure into a bulk material [2]. In turn, the gradation processes can be classified as constitutive, homogenizing, or segregating, depending on the manufacturing process. FGMs produced by DLD have a constitutive gradation process. The graded structure is gradually built up by the precursor materials (usually the powders), and the consolidation process occurs almost simultaneously. DLD is the technology that makes it possible to manufacture a greater variety of FGMs in a single step and is the result of advances in additive manufacturing technology that made it technologically and economically viable.

Table 1 presents an overview of the materials used in the production of FGMs in different studies, as well as the main results and expected applications for these innovative materials.

From the analysis of Table 1, the importance of steels as a substrate material is highlighted. This is related to the industrial implementation of steels and the ability of FGMs to improve the behavior of gears. As for the material of the FGMs, the highlight goes to nickel superalloys, steels and, in general, materials that can provide high hardness and resistance to wear or other surface degradation processes.

The selection of austenitic stainless steel (316L or 304L) as the material of choice for the substrate is due to the fact that this material does not undergo martensitic transformation unless under very special conditions, such as cryogenic treatments. Thus, this steel withstands the melting of a superficial layer of the substrate, the rapid expansion and contraction that substrate suffers, and the high cooling rates from high temperatures usually imposed on the substrates, without significant microstructural changes. This allows it to minimize one of the main problems in using DLD, which is the appearance of high residual stresses in both the clad and the substrate.

In fact, producing FGMs requires an understanding of thermal and thermophysical properties: coefficient of thermal expansion (CTE), melting temperature, and thermal conductivity. The inequality in the heat flow is due to its faster dissipation at the material interface that presents higher thermal conductivity, resulting in distortion and the possibility of lack of fusion in the material with lower thermal conductivity, promoted by insufficient heat [32].

High residual stresses in FGMs can be due to the thermal expansion differences and to lattice misfit. In DLD, the extremely high thermal gradient enhances thermal stresses; these are related with the expansion associated with the melting pool and the contraction during rapid cooling [33]. These mismatches can arise between the first layers of the FGM and the substrate and through the FGM and be the cause of cracking or interfacial delamination between the clad and the substrate or between the FGM layers. The distribution of these stresses is highly dependent on the substrate and on the FGM materials and can be tensile on the substrate and compressive on the FGM or vice versa. However, experimental and numerical results have proven that increasing the number of layers, with a composition gradient to reduce the CTEs difference and lattice misalignment, can minimize this effect [34,35]. The thickness and composition of each layer are also critical factors in the residual stress profile [36]. Processing conditions are also determinant in the magnitude of residual stresses, this being particularly important in processes such as DLD in which thermal energy is transferred

to the cold substrate quickly. For example, in the deposition of an Fe-V-Cr powder (CPM 9V) on tool steel (H13), it was observed that the normal residual stresses increase with an increase in laser power and decrease with an increase in scanning speed [37].

Preheat treatment is a solution to relieve the residual stresses in FGMs. Preheating reduces the thermal mismatch between the melt pool and the solid material (substrate or newly solidified clad), thus decreasing the cooling rate of both the substrate and the cladding and the formation of residual thermal stresses [38-40]. The slower cooling rate also prevents the formation of brittle phases in the FGM and in the substrate, minimizing the likelihood of cracking. In steels, increasing preheat temperature prevents the formation of brittle martensite and can promote bainite decomposition and increase the percentage of ferrite, leading to a reduction of hardness and residual stresses [41].

Table 1: General description of FGM fabricated by DLD.

Substrate	FGM Materials	Functionality (Applications?)	Main Results	Reference
Carbon steel	SS316L Inconel 718	FGM for wear-resistance applications.	Production of linear FGMs, presenting a microstructure with a transition from columnar to equiaxial. Increased resistance to wear.	[42]
Carbon steel	Inconel 690 TiC	Test pieces.	The addition of TiC changes the microstructure of the Inconel 690 matrix, presenting a refinement of grains, and promoting a significant increase in hardness and wear resistance.	[21]
Carbon steel	SS 316L CrCo alloy (Stellite 6)	Aeronautical and biomedical industries.	Development of a process modelling and a system control to manufacture FGM parts. Comparison with experimental results.	[1]
Carbon steel	Fe-16Ni-4Cr Fe-21Cr-8Ni	Fabrication of gear parts.	Three different powders were used to build a gear with a hardness gradient between the inner region (lower hardness) and the outer region (greater hardness), which is in contact with other structures. The FGM was easily produced using the DLD technique.	[43]
Carbon steel	SS 316 Fe	Test Pieces	The FGM deposited on the mild steel showed a reduction in the number of defects (pores and cracks) compared to the direct deposition of SS316.	[24]
Carbon steel (A516) Inconel 718	YSZ (ZrO2, 8 YSZ) NiCrAlY Inconel 625	Thermal barrier claddings	The residual stresses distribution through the layers of a functionally graded cermet were modelled. The model was validated using two FGMs.	[34]
Carbon steel (SAE387 Gr22)	Fe-2.25Cr Pure iron Pure chromium	Applications in superheater tubes and vessels of nuclear energy generation facilities.	FGM transition joints promoted the control of carbon diffusion across dissimilar alloys for nuclear energy applications	[44]
Carbon steel	SS 316L Ferritic steel (P21)	Test Pieces	In a multilayered material, the FGM region presented superior mechanical properties such as continuous yielding, higher tensile strength, and higher work-hardening rate than the austenitic and ferritic steel layers.	[45]
Carbon steel	SS 420/V/Ti6Al4V Ti6Al4V/V/SS304L SS 420/V	Dissimilar materials for aerospace and nuclear industries.	The formation of the fragile σ FeV phase in FGMs was investigated. This phase, associated with cracking, has a minimal amount in SS420/V/Ti6Al4V FGM's.	[46]
SS 316L	SS 316L Inconel 718	Test Pieces	The tensile strength of FGMs is inversely proportional to laser power and proportional to powder feed rate. The formation of NbC allowed the control of hardness and increased wear resistance.	[47]
SS 316L	Inconel 625 SS 316L	Test Pieces	FGM produced with Inconel 625, and SS316L powders showed mechanical resistance and hardness like SS 316L substrate.	[48]
SS 316L	SS 316L Co-superalloy	Industrial and biomedical components	FGMs were produced gradually changing the proportions of both precursors. The mechanical properties and microstructure show the same trend, evolving from those typical of the SS 316L to the ones of the Inconel 718.	[49]
SS 316L	SS 316L SS 630 (17-4PH)	Industrial and medical components	FGM was successfully produced without defects such as cracks and porosity. Hardness increased with the amount of 17-4PH steel.	[50]
SS 316L	SS 316L Ni-Cr-B-Si	Dissimilar materials joints.	Fabricated FGMs show that compositional variation causes a smooth gradient in properties such as hardness, ductility, and energy storage ability. Heat treatment significantly affects the microstructure and mechanical properties of FGMs.	[51]

SS 316L	SS 316L Inconel 625 Ti6Al4V	Components that require both high corrosion resistance and a high strength-to-weight ratio.	Synchronous preheating proved to be fundamental for the production of crack-free FGMs by altering the formed phases.	[52]
SS 304L	SS 304L Inconel 625	Extreme-environment applications such as in aerospace or nuclear power generation.	Cracks were observed in the gradient zone and are associated with small amounts of transition metal carbides particles.	[7]
SS 304L	SS 316L Inconel 625	Engineering fields: aerospace, biological, nuclear and photoelectric.	FGMs with continuous composition gradient show strong metallurgical bond between each deposition. Wear resistance increased with increasing Inconel 625 amount. Higher hardness was obtained for 50% Inconel 625 + 50% 316L..	[3]
SS 304L	SS 316L Inconel 625 (50%/50%)	Test Pieces	The FGM has been successfully produced with no defects. Yield strength and tensile strength of FGMs are close to that of pure Inconel 625 and pure SS 316L, respectively.	[53]
AISI 304L	SS 316L Inconel 728	Components to harsh situations, such as nuclear power plants and oil refineries.	The brittle Laves phase was detected when the content of Inconel 718 exceeded 40 %. The fracture mechanism of the FGMs was the microporous aggregation fracture, induced by the Laves phase.	[54]
Nodular cast iron	Inconel 625 SS 420	Repair of components for different industries.	Repair of nodular cast iron structures using FGM's is appropriate. The FGM has good wear resistance.	[55]
Inconel 718	NiCrSiBC WC	Protective ceramic-metal composite coatings.	Controlling process parameters did not prevent cracking. Crack-free coatings could only be obtained by pre-heating the substrate (300 °C and 500 °C).	[40]
Ti6Al4V	Ti6Al4V Mo Inconel 718	Test Pieces	The importance of using a buffer material (transition layer) and controlling the different cooling speeds of the FGM materials to obtain a sound FGM is emphasized.	[56]
TI6Al4V	TI6Al4V Ti48Al2Cr2Nb	Materials for blisks of turbine blades (Ti48Al2Cr2Nb) and turbine disks (TI6Al4V) on aero engines.	FGM without cracks or metallurgical defects has been successfully manufactured. FGM reduces the sensitivity to cracking, particularly in titanium aluminide.	[57,58]

Solidification and Microstructure Formation

The functional properties and quality of claddings produced by DLD are strongly dependent on the final microstructure. Rapid solidification in additive manufacturing can lead to solute segregation and the formation of unwanted, and unexpected, brittle phases. In fact, the DLD process promotes very high cooling rates, in the range of $5x10^3$ - 10^6 K/s, and diffusive transformations in the solid-state are usually suppressed. For this reason, homogenisation and control of the solidification process are fundamental to obtain the desired microstructure. Thus, one of the prerequisites for a successful process is homogenizing the melt in each layer. Several physical phenomena act in the melt pool; however, the fluid flow is dominated by Marangoni convection [59-61]. The melt pool is well-mixed due to this intense Marangoni convection that directly affects the shape and penetration of the pool, the chemical composition, the microstructure, and therefore the final properties of the FGM [62-64]. This convection, in which the surface tension gradient drives the material flow, also determines the formation of defects, such as porosities and cracks [61,65-68].

Process parameters and material properties influence the Marangoni convection [61,66]. An example is shown in Figure 3, which presents computed results evidencing the influence of laser scanning speed on liquid velocity; as the speed increases, the maximum liquid velocity moves from the sides to the rear of the pool, affecting the extension and the shape of the liquid pool [66]. This directly influences the microstructure, as illustrated in Figure 4, which shows EBSD images of a Ni superalloy processed with three different scanning speeds.

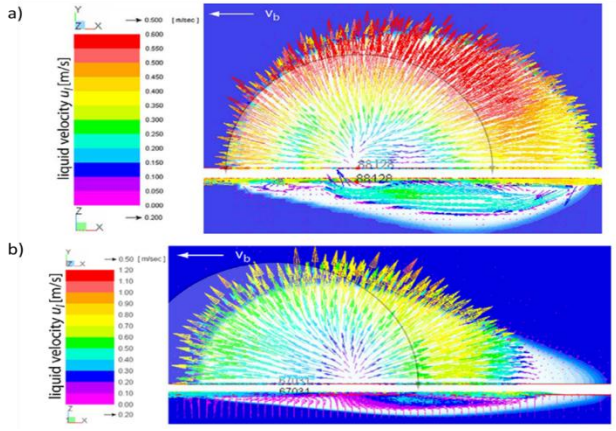

Figure 3: Simulation of Marangoni convection. The figures represent computed liquid pool and flow fields for two scanning speeds: (a) 3.5 and (b) 100 mm/sec [66].

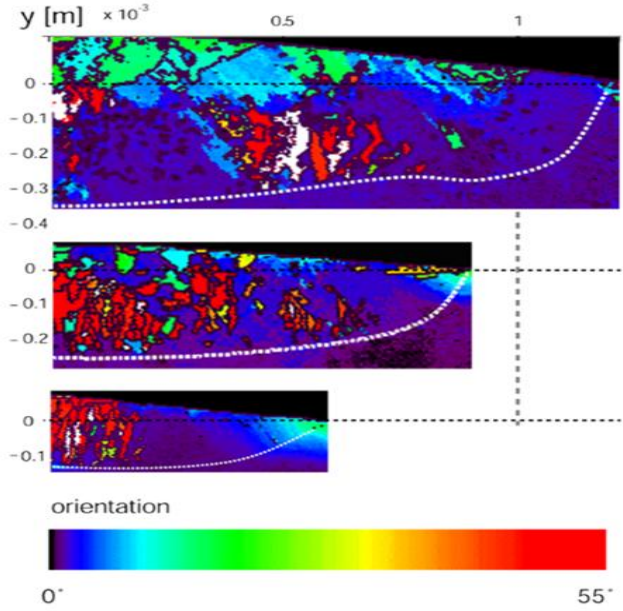

Figure 4: EBSD maps for three scanning speeds [66].

Another example of the influence of processing parameters is shown in Figure 5. The cross-section analysis shows the

influence of laser power on the shape and dimensions of the melt pool, modification of grain orientations, layer thickness, and surface finishing. All these modifications are direct effects of the influence of laser power on Marangoni flow [69].

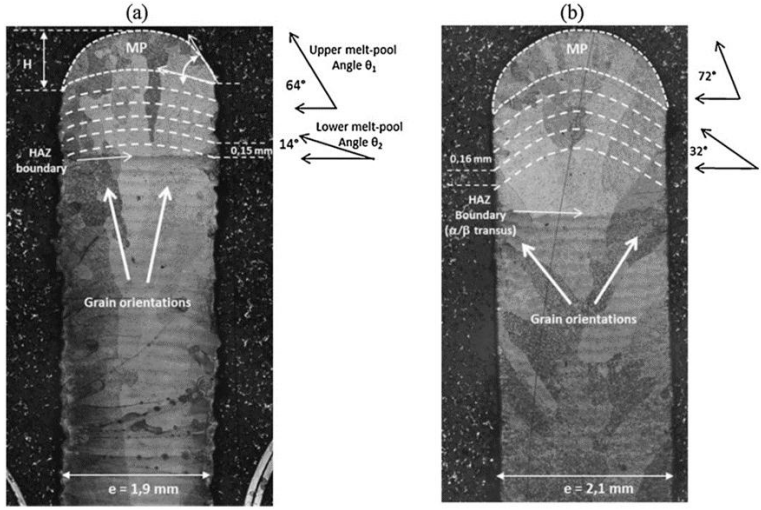

Figure 5: Influence of laser power on the microstructure of Ti6Al4V clads. Cross sections of clads produced with laser powers of (a) 320 W and (b) 500 W [69].

Figure 5 is a typical microstructure of a clad produced by DLD. In this process, the solidification modes evolve rapidly due to changes in solidification rate (R) and temperature gradient at the solid-liquid interface (G). These changes lead to the development of different microstructures that can be observed in laser additive manufacturing [68,70,71]. For a given alloy, the microstructure depends on the local solidification conditions. Specifically, the morphology of rapidly solidified layers is controlled by the G/R parameter. If G/R is greater than a critical value, a planar solidification front occurs, while if G/R is smaller than this critical value, the planar solid-liquid interface is destabilised, and cellular or dendritic solidification occurs [60,68,72].

At the beginning of the solidification, the planar solidification zone appears at the bottom of the melt pool, where the liquid

metal maintains contact with the solid substrate (solidification rate is 0, and the G/R is infinite). With the propagation of the solid-liquid interface, R rapidly increases, and G decreases, leading to a lower G/R value: the planar front evolves into a cellular interface and eventually to a dendritic one when G/R decreases even more. In the DLD process, due to the fast variation of G/R, the planar zone is very narrow [61,73,74], as seen in Figure 6.

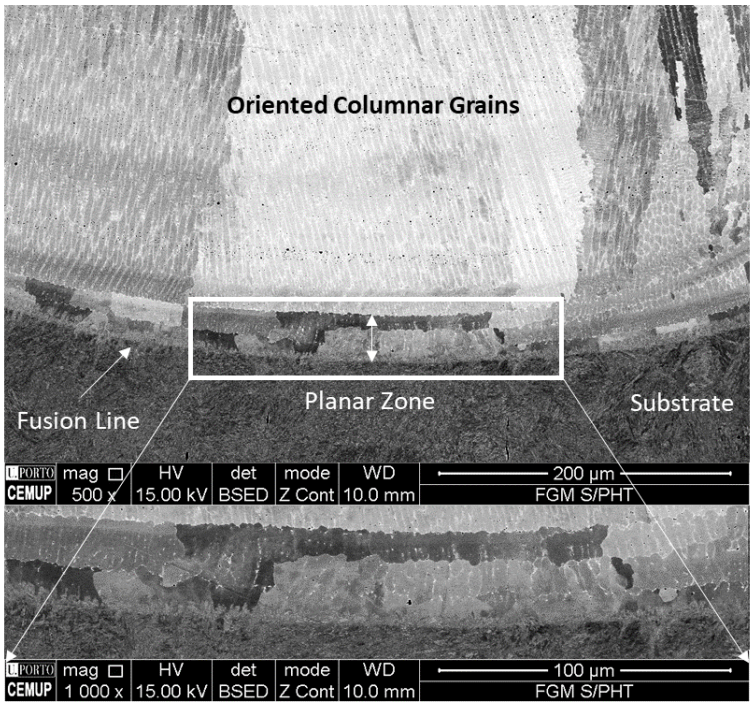

Figure 6: SEM micrograph of the cross section of a layer of Inconel 625 deposited on 42CrMo4 steel in which the planar zone and columnar grains can be observed.

With the evolution of the solidification process, the decrease in G/R slows down until reaching a value that remains practically constant. In this region, which follows the cellular interface zone, dendritic solidification appears. Cellular and dendritic solidifications are generally columnar and grow perpendicular to the substrate/solidified layers. This is due to the rapid heat

dissipation by the substrate and solidified layers, the thermal gradient being higher in this direction. Near the surface of the cladding layer, heat is also dissipated through the surrounding atmosphere, which significantly decreases the G value. In this region, dendrites become very thin and disoriented [61,73,75]. For a detailed description of G and R influence in solidification modes and microstructure development, see, for instance [76,77].

The laser processing conditions and the clad building direction are factors that influence the microstructure and, therefore, the functional properties of claddings [78,79].

In FGMs with composition gradients, the microstructure is also influenced by different materials characteristics, making solidification control more complex. An example of the microstructure formed in FGMs materials with a gradual change in composition is present in Figure 7. This figure shows the microstructure of an Inconel 625/ NiCrWMo superalloy (D4006) FGM. The first layers deposited are 100% Inconel 625, which gradually changes up to 100% D4006. Three intermediate zones have been sequentially deposited (75% Inconel 625 + 25% D4006, 50% Inconel 625 + 50% D4006, 25% Inconel 625 + 75% D4006).

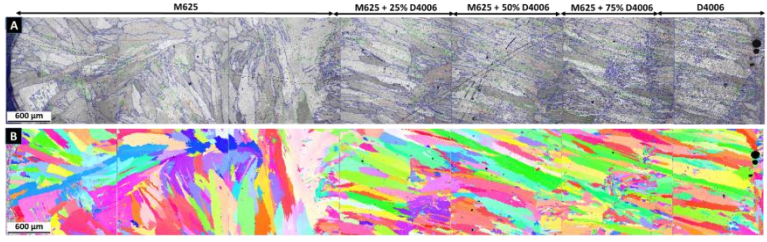

Figure 7: SEM images of the microstructure of an Inconel 625 (M625)/ NiCrWMo superalloy (D4006) FGM. (a) Microstructure evolution along the FGM, and (b) EBSD inverse pole figures (IPF).

From the analysis of the figure, some columnar grains that cross several layers stand out. These grains do not seem to be influenced by compositional changes, indicating the possibility of epitaxial growth. This type of microstructure occurs because the deposition of a new layer implies the remelting of part of the

previous one, allowing the grains to function as nucleation sites for subsequent solidification. Despite this epitaxial growth, the IPF images do not show the formation of a strong preferential orientation (texture).

Defects

The most frequently detected defects in claddings produced using the DLD technique are cracks [80], porosity [81], chemical segregation [82], formation of intermetallics [83], and unmelted powder particles [84], all of which promote the deterioration of the mechanical properties of the components. Some of these defects, even if of a submicrometric dimension, can have serious consequences. In fact, micro segregation, and the formation of brittle phases, like intermetallics, enhance the nucleation of microcracks, leading to component collapse. Defect reduction is therefore essential so that the FGMs do not fail in service.

The main causes of the development of defects are associated with processing parameters, as in most manufacturing processes. Laser power, powder feed rate, scanning speed, and powder particle size are factors that can promote cracking and pore formation. The optimization of processing conditions will allow a good metallurgical bond between the deposit and the substrate, and an adequate dilution. Dilution is an essential aspect of DLD clads and assesses the contribution of the substrate area that is melted by the laser to the total area of the clad, controlling clad contamination by the substrate and affecting the deposition yield. This optimization minimizes defects such as cracks and porosities, which can act as stress concentrators and nucleate fatigue cracks [29,85]. For some materials, it has been shown that increasing laser power intensifies residual stresses, cracks formation, and the deterioration of mechanical properties [33,86].

The formation of cracks can also be associate with phases that locally introduce high discontinuity in the hardness, brittleness, and thermal stability of the FGMs (see Figure 8). Attention has been paid to the formation of intermetallic compounds [58],

eutectics (low melting point) and borides [87], and Laves phase [82,88-93].

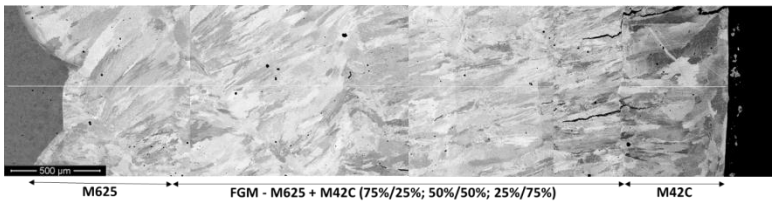

Figure 8: SEM images of the microstructure of an Inconel 625 (M625)/martensitic stainless-steel (M42C) FGM showing cracking formation in the 25% Inconel 625 + 75% M625 layer.

The formation of the Laves phase in nickel-based superalloys has been widely studied since this material is one of the most manufactured using DLD, including in the production of FGMs. The brittle intermetallic Laves phase is formed due to the interdendritic segregation of chemical elements of the matrix. This phase is a product of the eutectic reaction, $L \rightarrow (\gamma + \text{Laves})$, is dependent on local elements concentration during non-equilibrium solidification [84,90], and leads to the reduction of useful alloying elements (Ni, Fe, Cr, Nb, Mo, Ti) in the matrix, as shown in Figure 9 for niobium. The formation of Laves phase is highly undesirable, as it deteriorates the mechanical properties of the cladding, such as ductility, tensile strength, and fatigue life [88,92]. Furthermore, it increases the susceptibility to hot cracking [89]. The amount of this phase is higher in FGM regions processed with higher energy density [91]. A high cooling rate promotes less redistribution of elements, forming larger Laves phase particles, with a detrimental effect in mechanical response [82,92]. The addition of vanadium inhibits niobium segregation, thus reducing Laves phase formation, positively influencing the microstructure. In addition, vanadium changes the morphology of the Laves phase from a rod-like to particle-like shape [93].

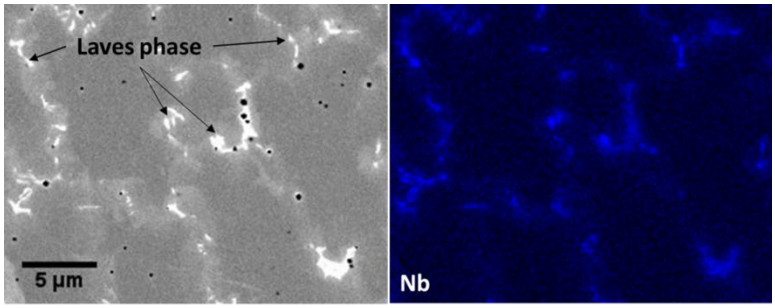

Figure 9: SEM images showing the morphologies of Laves phase particles and Nb element distributions in the interdendritic regions.

Porosity is another extremely harmful defect to the performance of the FGMs. It is mainly the result of gases encapsulated in the powder feed system or powder particles and by an inadequate selection of process parameters [22,81,85]. Porosity may also be associated with high melt pool cooling rates [94].

Unmelted powder particles are another defect that induces the degradation of FGMs performance. This defect is formed due to insufficient energy density, causing low absorption of laser energy and promoting the non-fusion of the powder, favouring the formation of cracks due to low metallurgical bond [95,96]. In the production of FGMs, this problem increases since the different powders have different thermophysical properties [56].

One procedure that promotes the reduction of residual stresses and defects, such as cracks, is the preheating of the substrate and the maintenance of this preheating during the deposition process [56]. Preheating also inhibits the formation of harmful phases such as eutectics and borides [87], thus reducing defects in FGMs. Preheating is also essential in controlling thermal gradients between the substrate and the deposited layers, by decreasing the cooling rate and residual stresses [40,97] and attenuating the difference in thermal expansion coefficients between the several powders [58], thus inhibiting the formation of cracks and promoting better mechanical properties.

In summary, to overcome the current challenges to FGMs production by DLD on different substrates, it is necessary to

develop integrated methodologies that consider and integrate all processing phases, such as parameter definition, process optimization, and thermomechanical simulations.

Mechanical Characterisation

Undoubtedly, one of the main objectives of the production of FGMs is to obtain different mechanical properties from the combination of materials. Another objective is to ensure gradual and crack-free transition between substrate and last cladding layers, which also translates into the variation of mechanical properties. This section highlights some of the most important mechanical properties of several FGMs, such as microhardness, tensile properties, and wear resistance. As already mentioned, one of the main groups of FGMs produced results from combinations of steels with nickel superalloys. This review of the mechanical properties of FGMs begins with the analysis of this combination.

An FGM with a composition gradient between pure stainless-steel 316L (SS316L) and pure Inconel 718 (IN718), with three intermediate layers (25%, 50%, and 75 of IN718) deposited on SS 316L was manufactured [47]. The influence of laser power (LP) and powder feed rate (FR) on the mechanical performance of the material was studied. Crack-free FGMs were produced for the four laser powers and two feed rates tested. Tensile tests on the specimens revealed reduced ductility with the fracture starting in the steel. The tensile strength decreases with the increase in laser power and the decrease in the feed rate, being 596 MPA for LP = 450 W and FR = 0.834 g/s and 527 MPa for and LP = 750 W and FR = 0.632 g/s.

The Vickers microhardness analysis along the FGM shows an approximately parabolic hardness distribution with an initial decrease as the amount of steel decreases, a minimum for the layer with an equal amount of both powders and increasing to a maximum corresponding to the last layer of pure Inconel, the only non-reheated layer [47]. As with tensile strength, an increase in laser power leads to a decrease in hardness.

The Mean Specific Wear Rates (MSWR) of constant composition layers, produced with the four laser powers and the two powder feed rates, were also determined [47]. MSWR is lower in pure steel for all conditions, goes through a maximum for the 75% SS 316L + 25% Inconel 718 composition, and decreases with the increasing amount of Inconel. The highest MSWR values were obtained for the highest laser power and lower feed rate.

This evolution of the mechanical properties, related to the spacing of the secondary dendritic arms and carbide formation, shows that tailored mechanical properties can be obtained by optimizing the processing parameters and composition, allowing the adequate selection to fulfil the FGMs requirements.

The SS316 L/Inconel718 FGM with different composition gradients were also fabricated by DLD [54]. The composition changed from pure SS316L to pure IN718, increasing by 5%, 10%, or 20% the IN718 amount every ten layers. This composition gradient affects the mechanical response of the FGMs. The fracture of the tensile sample occurred at layers corresponding to 20–40%, 50–60%, and 25%–30% IN718, for the composition gradients of 20%, 10%, and 5%, respectively. The best tensile properties, with the highest tensile strength (527 MPa) and the highest elongation (26%), were obtained by the FGM with a composition gradient of 10 %. These results evidenced that the gradient variation is essential for FGMs fabricated by additive manufacturing.

316L stainless steel (SS316L) and Inconel 625 (IN625) powders have also been mixed to make FGMs [98]. In this study, FGMs produced with an abrupt transition between SS316L and IN625, and with a transition zone, where the relative amount of IN625 gradually increases by 12.5% every two layers, were analysed. Mechanical properties were compared with those of pure materials produced under the same conditions.

The mechanical response of the FGMs was determined by the softest material (SS316L) and, assuming that the toughest IN625 has negligible plastic deformation, the tensile properties of both

FGMs are almost identical to those of SS316, with no noticeable differences in mechanical strength and ductility [98]. This means that, in this case, a good interfacial resistance between the two materials has been achieved and the transition zone, which makes the manufacture of the FGM much more complex, is not necessary. Recently, another SS316L/IN625 FGM, deposited on the same substrate (SS304), was produced with other processing conditions, and the mechanical properties were investigated [3]. The FGM produced had a transition zone in which the relative amount of IN625 increased by 10% in each region. In this FGM the tensile specimens also showed a noticeable plastic deformation and ductile fracture. An analysis of the fracture surfaces indicated that the fracture occurred in layers with 60% SS316L + 40% IN625. In this analysis, particles rich in Nb were detected at the bottom of the dimples, indicating that fragile particles resulting from the segregation of this element, eventually phase Laves, maybe at the origin of the fracture.

The average yield strength obtained for five samples were 823 MPa and the average tensile strenght 1030 MPa [3]. These values are much higher than the average values reported in [98] (310 and 540 MPa for yield strength and tensile strenght, respectively) and even higher than typical of 316L stainless steel.

The microhardness along the transition zone showed a gradual upward trend, with a maximum of 347 HV for the deposited layer with 50% SS316L + 50% IN625. The wear of samples with various compositions was also analyzed. It was determined that the wear resistance first decreases slightly with an increasing percentage of IN625 but then increases significantly, approaching that of the superalloy for 20% SS316L + 80% IN625 (as can be seen in the Table 2) [3].

Table 2: Wear rate for FGM samples and pure materials [3].

Sample composition	Wear rate ($x10^{-3}cm^{-3}.N.m^{-1}$)
100% SS316l	1.58
80% SS316L + 20% IN625	1.60
60% SS316L + 40% IN625	1.32
40% SS316L + 60% IN625	1.15
20% SS316L + 80% IN625	0.79
100% IN625	0.74

The microhardness evolution of an FGM fabricated using two nickel superalloys powders, Inconel 625 (IN625) and NiCrWMo (D4006), is shown in Figure 10. This FGM has five different regions; the first layers of the FGM were 100% IN625, and the amount of the NiCrWMo superalloy increase by 25% in each of the three intermediate regions, ending the deposition with 100% NiCrWMo. The microhardness increase as the amount of NiCrWMo powder is increasing. This factor is related to the strengthening effect of alloying elements (Cr, W, Mo).

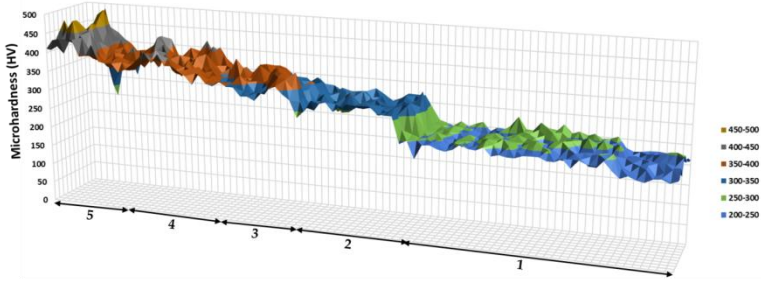

Figure 10: Vickers microhardness mapping of an FGM along the sample. The composition of the regions is: 1 - 100% IN625; 2 - 75% IN625 + 25% NiCrWMo; 3 - 50% IN625 + 50% NiCrWMo; 4 - 75% IN625 + 75% NiCrWMo; 5 - 100% NiCrWMo.

Another group of FGMs that has been studied a lot is the one that uses Ti6Al4V powders and powders of a much harder material. An example is a FGM deposited by DLD on a Ti6Al4V substrate, with composition changing from 100% Ti6Al4V to 50% Ti6Al4V + 50% TiC, and with a gradual increase in composition of 5% TiC in each zone [99]. One FGM was produced with constant processing parameters (FGM A) and the other with parameters optimized for each condition (FGM B). The results presented in Table 3 showed that the optimized FGM has the best wear-resistance behaviour, with a reduction of 82.5% in the wear volume compared with the substrate. The last layers of this FGM (with a composition of 50% Ti6Al4V + 50% TiC) has a microhardness value (1200 VHN) which is four times that of the Ti6Al4V.

Table 3: Wear volume for FGMs and substrate [99].

Sample designation	Wear volume (mm^3)
FGM A	0.033
FGM B	0.021
Substrate	0.120

These results show how the proper selection of the processing conditions for each zone (each composition) can be decisive in obtaining an optimized FGM behaviour.

Ti6Al4V/TiC FGM production with a 1% TiC increase in each of the 50 layers of up 50% TiC has also been tested [100]. The FGM microhardness gradually increases from 380 HV in the Ti6Al4V layer to 737 HV in the top layer (with 50% TiC), which means it almost doubles. This hardness variation is less important than reported in [99], emphasizing the effect of processing parameters and powders characteristics.

To analyse the tensile properties of this Ti6Al4V/TiC FGM, samples with fixed composition were deposited (each sample was the result of the deposition of ten layers). Six compositions were produced, with 0, 10, 20, 30, 40, and 50% TiC. The last two compositions were not tested as cracks appeared during the FGMs production. The ultimate tensile strength of the FGM with a TiC amount of 5% is improved by 12% compared to Ti6Al4V. Contrary to what was expected considering the hardness evolution, further increase of the TiC amount decreases the tensile strength, and the elongation drops to less than 1%. This unexpected behaviour was explained by increasing unmelted TiC particles and dendritic TiC phases, which promote premature damage of FGMs [100].

The brittleness of the Ti6Al4V/TiC FGM is a problem that should be carefully considered during its manufacture by DLD technology. The effect of laser power and scan speed on hardness of Ti6Al4V/TiC FGM deposited in a Ti6Al4V substrate was analyzed [101]. FGMs were deposited with increase of TiC through three zones, with 10, 20, and 30% TiC, and laser power ranging from 400 to 700 W and scan speeds of 200, 300, and 400 mm/min. The Vickers hardness gradually increases from 300 HV

to 600 HV with the increase of TiC amount. No significant differences were observed for the set of processing parameters tested. Samples with constant composition (0, 10, 20, and 30% TiC) were produced for tensile tests [101]. Ultimate tensile strength and elongation decreases with increasing TiC amount, being this more noticeable for 20 and 30% TiC, which confirms the results reported in [100].

Ti6Al4V and Invar 36 (64 wt% Fe, 36 wt% Ni) powers were used to produce an FGM [102]. The FGM started with the deposition of 21 layers of Ti6Al4V powder onto a Ti6Al4V substrate, followed by a 32 layers gradient region with a 3% decrease in Ti6Al4V per layer (replaced by 3% Invar powder), and, finally, 22 layers of pure Invar. Hardness shows a noticeable increase for layers with 40-60% Invar. In these layers, values close to 900 HV were measured, being much higher than the average values of Ti6Al4V and Invar, which are 380 and 141 HV, respectively. These significantly higher hardness values were associated with the formation of iron and nickel titanides in the FGM. These intermetallic phases are very hard but also very brittle, which may explain the macroscopic cracking of the FGM. Although hardness values measured in the FGM central region are excellent, the defects preclude Ti6Al4V/Invar from being used in industrial applications.

Ti/SiC was another metal/ceramic FGM produced by DLD with a combination of powders similar to the one described above, a ductile titanium alloy gradually reinforced with a carbide. In this FGM, a layer of 100% Ti was first deposited on a Ti6Al4V substrate, then eight more layers were deposited with a constant decrease of 10% Ti (an increase of 10% SiC), with the final layer having the composition of 20% Ti + 80 % SiC [103].

One of the main challenges of these FGMs is to successfully achieve a high volume content of the ceramic constituent at the exterior layer, surmounting the problems caused by the great brittleness and the poor melting fluidity of most ceramics. To achieve this goal, the composition and thickness of the Ti/SiC FGMs layers were optimized, first eliminating the layers with a greater tendency to cracking (namely the layer with 70% Ti +

30% SiC), and then halving the thickness of the layers. After this optimization, it was possible to avoid forming the more cracking and microcracking inducing phases and producing an FGM without evident defects. In this optimized FGM, the hardness continuously increases from 339 HV in the Ti layer to 1608 HV in the outer layer (10% Ti+90% SiC), and average three-point bending strength of 286 MPa was measured at room temperature [103].

These mechanical properties show that it is possible to produce metal/ceramic FGMs with the proper selection of the layer construction strategy. In summary, some aspects related to mechanical properties can be highlighted:

- Final mechanical properties are not necessarily a combination of the mechanical properties of the materials used in the FGM and may vary significantly across the deposited zone.
- The variation of mechanical properties along the FGM is not necessarily gradual or linear and is strongly related to the microstructure.
- In some cases, defects induced by the FGM process, such as cracks and porosities, can negatively affect the mechanical properties, making its industrial application unfeasible.
- The production of FGMs has often proven to be able to improve mechanical properties such as wear-resistance and hardness.
- The deposition parameters, including the composition and thickness of the various layers, play a significant role in the final properties and must be optimized to achieve the intended requirements.

Conclusions

Functional Gradient Materials (FGM) combine materials with different compositions, leveraging the best properties of each and exploring reactions that can give rise to unexpected properties. FGMs respond to the growing demand from various industrial sectors for materials with better performance, allowing them to produce components with unique characteristics and a

gradient of properties along a specific direction. The production of FGMs by Direct Laser Deposition (DLD) is an attractive solution for many engineering applications, thus opening new perspectives for several industrial sectors, such as aerospace, automotive, nuclear, and biomedical. In this review, the current status of research on using the DLD process for manufacturing FGMs has been summarized. The main characteristics of this manufacturing process, the microstructures and mechanical properties of FGMs, and their main defects, were described. DLD is the technology that makes it possible to manufacture the widest range of FGMs and results from additive manufacturing progress that makes it technologically and economically viable. This process provides freedom to design more complex components, built layer by layer, with strategically controlled compositional variations that enable the directionality of properties. The production of FGM by DLD has been widely used as it opens up the possibility of blending different types of materials, such as metals (steel, superalloys, and titanium alloys) and ceramics. This review also highlights the need for more studies in producing these materials, expanding the analyzed systems, optimizing processing conditions, and properly establishing the correlation of microstructures, phase changes, and defects with the properties of the FGM, thus enhancing its performance in service.

References

1. P Muller, P Mognol, JY Hascoet. Modeling and control of a direct laser powder deposition process for Functionally Graded Materials (FGM) parts manufacturing. J. Mater. Process. Technol. 2013; 213: 685–692.
2. B Kieback, A Neubrand, H Riedel. Processing techniques for functionally graded materials. Mater. Sci. Eng. A. 2003; 362: 81–106.
3. B Chen, Y Su, Z Xie, C Tan, J Feng. Development and characterization of 316L/Inconel625 functionally graded material fabricated by laser direct metal deposition. Opt. Laser Technol. 2020; 123.
4. HP Qu, P Li, SQ Zhang, A Li, HM Wang. Microstructure and mechanical property of laser melting deposition (LMD)

Ti/TiAl structural gradient material. Mater. Des. 2010; 31: 574–582.
5. X Lin, TM Yue, HO Yang, WD Huang. Microstructure and phase evolution in laser rapid forming of a functionally graded Ti-Rene88DT alloy. Acta Mater. 20006; 54: 1901–1915.
6. RM Mahamood, ET Akinlabi. Laser Additive Manufacturing. 2016.
7. BE Carroll, RA Otis, JP Borgonia, J Suh, RP Dilon, et al. Functionally graded material of 304L stainless steel and inconel 625 fabricated by directed energy deposition: Characterization and thermodynamic modelling. Acta Mater. 2016; 108: 46–54.
8. C Petit, L Montanaro, P Palmero. Functionally graded ceramics for biomedical application: Concept, manufacturing, and properties. Int. J. Appl. Ceram. Technol. 2018; 15: 820–840.
9. N Radhika, K Teja, K Rahul, A Shivashankar. Fabrication of Cu-Sn-Ni /SiC FGM for Automotive Applications: Investigation of its Mechanical and Tribological Properties. Silicon. 2018; 10: 1705–1716.
10. M Koizumi. FGM activities in Japan, Compos. Part B Eng. 1997; 28: 1–4.
11. M Soodi, SH Masood, M Brandt. Thermal expansion of functionally graded and wafer-layered structures produced by laser direct metal deposition. Int. J. Adv. Manuf. Technol. 2013; 69: 2011–2018.
12. Y Li, Z Feng, L Hao, L Huang, C Xin, et al. A Review on Functionally Graded Materials and Structures via Additive Manufacturing: From Multi-Scale Design to Versatile Functional Properties. Adv. Mater. Technol. 2020; 1900981.
13. A Saboori, G Piscopo, M Lai, A Salmi, S Biamino. An investigation on the effect of deposition pattern on the microstructure, mechanical properties and residual stress of 316L produced by Directed Energy Deposition. Mater. Sci. Eng. A. 2020; 780: 139179.
14. W Paatsch. Energy turnaround - a challenge for surface technology. Trans. {IMF}. 2016; 94: 228–230.
15. Y Gao, D Xiong, C Wang, Y Chen. Influences of laser powers on microstructure and properties of the coatings on

the AZ91HP magnesium alloy. Acta Metall. Sin. (English Lett. 2009; 22: 167–173.
16. J Chen, SH Wang, L Xue. On the development of microstructures and residual stresses during laser cladding and post-heat treatments. J. Mater. Sci. 2012; 47: 779–792.
17. SM Thompson, L Bian, N Shamsaei, A Yadollahi. An overview of Direct Laser Deposition for additive manufacturing; Part I: Transport phenomena, modeling and diagnostics. Addit. Manuf. 2015; 8: 36–62.
18. EP Cardozo, GR Pardal, S Ríos, S Ganguly, ASCM D'oliveira. Additive techniques to refurbish Ni based components. Soldag. e Insp. 2019; 24: 1–11.
19. Q Guo, S Chen, M Wei, J Liang, C Liu, et al. Formation and Elimination Mechanism of Lack of Fusion and Cracks in Direct Laser Deposition 24CrNiMoY Alloy Steel. J. Mater. Eng. Perform. 2020; 29: 6439–6454.
20. V Promakhov, A Zhukov, M Ziatdinov, I Zhukov, N Schulz, et al. Inconel 625/TiB 2 metal matrix composites by direct laser deposition. Metals (Basel). 2019; 9: 1–15.
21. JM Wilson, YC Shin. Microstructure and wear properties of laser-deposited functionally graded Inconel 690 reinforced with TiC. Surf. Coatings Technol. 2012; 207: 517–522.
22. A Dass, A Moridi. State of the art in directed energy deposition: From additive manufacturing to materials design. Coatings. 2019; 9.
23. L Yan, Y Chen, F Liou. Additive manufacturing of functionally graded metallic materials using laser metal deposition. Addit. Manuf. 2019; 31: 100901.
24. S Nam, H Cho, C Kim, YM Kim. Effect of process parameters on deposition properties of functionally graded STS 316/Fe manufactured by laser direct metal deposition. Metals (Basel). 2018; 8.
25. RM Mahamood. Laser Metal Deposition of Metals and Alloys. 2018.
26. GH Loh, E Pei, D Harrison, MD Monzón. An overview of functionally graded additive manufacturing. Addit. Manuf. 2018; 23: 34–44.
27. GH Loh, E Pei, D Harrison, MD Monzón. An overview of functionally graded additive manufacturing. Addit. Manuf. 2018; 23: 34–44, 2018.

28. DT Sarathchandra, S Kanmani Subbu, N Venkaiah. Functionally graded materials and processing techniques: An art of review. Mater. Today Proc. 2018; 5: 21328–21334.
29. KF Walker, JM Lourenço, S Sun, M Brandt, CH Wang. Quantitative fractography and modelling of fatigue crack propagation in high strength AerMet®100 steel repaired with a laser cladding process. Int. J. Fatigue. 2017; 94: 288–301.
30. W Li, J Zhang, X Zhang, F Liou. Effect of optimizing particle size on directed energy deposition of Functionally Graded Material with blown Pre-Mixed Multi-Powder. Manuf. Lett. 2017; 13: 39–43.
31. M Naebe, K Shirvanimoghaddam. Functionally graded materials: A review of fabrication and properties. Appl. Mater. Today. 2016; 5: 223–245.
32. A Reichardt. Additive Manufacturing of Metal-based Functionally Graded Materials. UC Berkeley. ProQuest ID: Reichardt_berkeley_0028E_17635. Merritt ID: ark:/13030/m5zh1phm. Retrieved from https://escholarship.org/uc/item/32h5c2vp, 2017. Available Online at: https://escholarship.org/uc/item/32h5c2vp.
33. S Zhou, X Zeng, Q Hu, Y Huang. Analysis of crack behavior for Ni-based WC composite coatings by laser cladding and crack-free realization. Appl. Surf. Sci. 2008; 255: 1646–1653.
34. A Bhattacharyya, D Maurice. Residual stresses in functionally graded thermal barrier coatings. Mech. Mater. 2019; 129: 50–56.
35. XC Zhang, BS Xu, HD Wang, Y Jiang, YX Wu. Modeling of thermal residual stresses in multilayer coatings with graded properties and compositions. Thin Solid Films. 2006; 497: 223–231.
36. KZ Uddin, B Koohbor. Gradient optimization of transversely graded Ti-TiB structures for enhanced fracture resistance. Int. J. Mech. Sci. 2020; 187: 105917.
37. P Kattire, S Paul, R Singh, W Yan. Experimental characterization of laser cladding of CPM 9V on H13 tool steel for die repair applications. J. Manuf. Process. 2015; 20: 492–499.

38. K Dai, XX Li, LL Shaw. Comparisons between thermal modeling and experiments: Effects of substrate preheating. Rapid Prototyp. J. 2004; 10: 24–34.
39. B Zheng, Y Zhou, JE Smugeresky, JM Schoenung, EJ Lavernia. Thermal behavior and microstructural evolution during laser deposition with laser-engineered net shaping: Part I. Numerical calculations, Metall. Mater. Trans. A Phys. Metall. Mater. Sci. 2008; 39: 2228–2236.
40. A Sadhu, A Choudhary, S Sarkar, AM Nair, P Nayak, et al. A study on the influence of substrate pre-heating on mitigation of cracks in direct metal laser deposition of NiCrSiBC-60%WC ceramic coating on Inconel 718. Surf. Coatings Technol. 2020; 389: 125646.
41. C Ding, X Cui, J Jiao, P Zhu. Effects of substrate preheating temperatures on the microstructure, properties, and residual stress of 12CrNi2 prepared by laser cladding deposition technique. Materials (Basel). 2015; 11.
42. X Liang, D Wu, Q Li, L Jiang. Laser rapid manufacturing of stainless steel 316L/Inconel718 functionally graded materials: Microstructure evolution and mechanical properties. Int. J. Opt. 2010; 2010: 1–6.
43. WJ Ji, YH Moon. Fabrication of functionally graded properties by direct laser melting of compositionally selective metallic powder. ICCAS 2015 - 2015 15th Int. Conf. Control. Autom. Syst. Proc. 2015; 1955–1957.
44. JS Zuback, TA Palmer, T DebRoy. Additive manufacturing of functionally graded transition joints between ferritic and austenitic alloys. J. Alloys Compd. 2019; 770: 995–1003.
45. DK Kim, W Woo, EY Kim, SH Choi. Microstructure and mechanical characteristics of multi-layered materials composed of 316L stainless steel and ferritic steel produced by direct energy deposition. J. Alloys Compd. 2019; 774: 896–907.
46. LD Bobbio, B Bocklund, A Reichardt, R Otis, JP Borgonia, et al. Analysis of formation and growth of the σ phase in additively manufactured functionally graded materials. J. Alloys Compd. 2020; 814: 151729.
47. K Shah, I ul Haq, A Khan, SA Shah, M Khan, et al. Parametric study of development of Inconel-steel

functionally graded materials by laser direct metal deposition. Mater. Des. 2014; 54: 531–538.
48. R Koike, I Unotoro, Y Kakinuma, T Aoyama, Y Oda, et al. Evaluation for mechanical characteristics of Inconel625-SUS316L joint produced with direct energy deposition. Procedia Manuf. 2017; 14: 105–110.
49. J del Val, A Arias-González, O Barro, A Riveiro, R Comesaña, et al. Functionally graded 3D structures produced by laser cladding. Procedia Manuf. 2017; 13: 169–176.
50. A Bayode, S Pityana, E Titilayo Akinlabi. Fabrication of stainless steel-based FGM by laser metal deposition. Hierarchical Compos. Mater. 2019; 55–72.
51. SM Banait, CP Paul, AN Jinoop, H Kumar, RS Pawade, et al. Experimental investigation on laser directed energy deposition of functionally graded layers of Ni-Cr-B-Si and SS316L. Opt. Laser Technol. 2020; 121: 105787.
52. W Meng, W Zhang, W Zhang, X Yin, L Guo, et al. Additive fabrication of 316L/Inconel625/Ti6Al4V functionally graded materials by laser synchronous preheating. Int. J. Adv. Manuf. Technol. 2019; 104: 2525–2538.
53. X Zhang, Y Chen, F Liou. Fabrication of SS316L-IN625 functionally graded materials by powder-fed directed energy deposition. Sci. Technol. Weld. Join. 2019; 24: 504–516.
54. Y Su, B Chen, C Tan, X Song, J Feng. Influence of composition gradient variation on the microstructure and mechanical properties of 316 L/Inconel718 functionally graded material fabricated by laser additive manufacturing. J. Mater. Process. Technol. 2020; 283.
55. Y Liu, F Weng, G Bi, Y Chew, S Liu, et al. Characterization of wear properties of the functionally graded material deposited on cast iron by laser-aided additive manufacturing. Int. J. Adv. Manuf. Technol. 2019; 105: 4097–4105.
56. A Thiriet, C Schneider-Maunoury, P Laheurte, D Boisselier, L Weiss. Multiscale study of different types of interface of a buffer material in powder-based directed energy deposition: Example of Ti6Al4V/Ti6Al4V - Mo/Mo - Inconel 718. Addit. Manuf. 2019; 27: 118–130.
57. R Ma, Z Liu, W Wang, G Xu, W Wang. Laser deposition melting of TC4/TiAl functionally graded material. Vacuum. 2020; 177: 109349.

58. R Ma, Z Liu, W Wang, G Xu, W Wang. Microstructures and mechanical properties of Ti6Al4V-Ti48Al2Cr2Nb alloys fabricated by laser melting deposition of powder mixtures. Mater. Charact. 2020; 164.
59. D Dai, D Gu. Thermal behavior and densification mechanism during selective laser melting of copper matrix composites: Simulation and experiments. Mater. Des. 2014; 55: 482–491.
60. TN Le, YL Lo. Effects of sulfur concentration and Marangoni convection on melt-pool formation in transition mode of selective laser melting process. Mater. Des. 2019; 179: 107866.
61. YS Lee, M Nordin, SS Babu, DF Farson. Influence of fluid convection on weld pool formation in laser cladding. Weld. J. 2014; 93.
62. YP Lei, H Murakawa, YW Shi, XY Li. Numerical analysis of the competitive influence of Marangoni flow and evaporation on heat surface temperature and molten pool shape in laser surface remelting. Comput. Mater. Sci. 2001; 21: 276–290.
63. B Bocklund, LD Bobbio, RA Otis, AM Beese, ZK Liu. Experimental validation of Scheil–Gulliver simulations for gradient path planning in additively manufactured functionally graded materials. Materialia. 2020; 11.
64. T DebRoy, HL Wei, JS Zuback, T Mukherjee, JW Elmer, et al. Additive manufacturing of metallic components – Process, structure and properties. Prog. Mater. Sci. 2018; 92: 112–224.
65. A Reichardt, AA Shapiro, R Otis, RP Dillon, JP Borgonia, et al. Advances in additive manufacturing of metal-based functionally graded materials. Int. Mater. Rev. 2020; 1–29.
66. JM Drezet, S Mokadem. Marangoni Convection and Fragmentation in LASER Treatment. Mater. Sci. Forum. 2006; 508: 257–262.
67. L Aucott, H Dong, W Mirihanage, R Atwood, A Kidess, et al. Revealing internal flow behaviour in arc welding and additive manufacturing of metals. Nat. Commun. 2018; 9: 1–7.
68. E Kannatey. Materials Processing Principles of Laser. 2009.

69. M Gharbi, P Peyre, C Gorny, M Carin, S Morville, et al. Influence of various process conditions on surface finishes induced by the direct metal deposition laser technique on a Ti-6Al-4V alloy. J. Mater. Process. Technol. 2013; 213: 791–800.
70. L Song, G Zeng, H Xiao, X Xiao, S Li. Repair of 304 stainless steel by laser cladding with 316L stainless steel powders followed by laser surface alloying with WC powders. J. Manuf. Process. 2016; 24: 116–124.
71. R Acharya, JA Sharon, A Staroselsky. Prediction of microstructure in laser powder bed fusion process. Acta Mater. 2017; 124: 360–371.
72. Z Gan, H Liu, S Li, X He, G Yu. Modeling of thermal behavior and mass transport in multi-layer laser additive manufacturing of Ni-based alloy on cast iron. Int. J. Heat Mass Transf. 2017; 111: 709–722.
73. Z Zhang, P Farahmand, R Kovacevic. Laser cladding of 420 stainless steel with molybdenum on mild steel A36 by a high power direct diode laser. JMADE. 2016; 109: 686–699.
74. Y Lee, M Nordin, SS Babu, DF Farson. Effect of Fluid Convection on Dendrite Arm Spacing in Laser Deposition. 2014.
75. S Bontha, NW Klingbeil, PA Kobryn, HL Fraser. Thermal process maps for predicting solidification microstructure in laser fabrication of thin-wall structures. J. Mater. Process. Technol. 2006; 178: 135–142.
76. JC Lippold. Welding metallurgy and weldability. 2014.
77. E Toyserkani, A Khajepour, S Corbin. Laser Cladding Laser Cladding. 2017; 11.
78. I Hemmati, V Ocelík, JTM De Hosson. Microstructural characterization of AISI 431 martensitic stainless steel laser-deposited coatings. J. Mater. Sci. 2011; 46: 3405–3414.
79. P Guo, B Zou, C Huang, H Gao. Study on microstructure, mechanical properties and machinability of efficiently additive manufactured AISI 316L stainless steel by high-power direct laser deposition. J. Mater. Process. Technol. 2017; 240: 12–22.
80. X Luo, J Li, GJ Li. Effect of NiCrBSi content on microstructural evolution, cracking susceptibility and wear

behaviors of laser cladding WC/Ni-NiCrBSi composite coatings. J. Alloys Compd. 2015; 626: 102–111.
81. C Zeng, W Tian, WH Liao, L Hua. Microstructure and porosity evaluation in laser-cladding deposited Ni-based coatings. Surf. Coatings Technol. 2016; 294: 122–130.
82. Y Chen, Q Zhang, Z Chen, L Wang, J Yao, et al. Study on the element segregation and Laves phase formation in the carbon nanotubes reinforced IN718 superalloy by laser cladding. Powder Technol. 2019; 355: 163–171.
83. JJ Candel, V Amigó, JA Ramos, D Busquets. Sliding wear resistance of TiCp reinforced titanium composite coating produced by laser cladding. Surf. Coatings Technol. 2010; 204: 3161–3166.
84. H Kim, W Cong, HC Zhang, Z Liu. Laser engineered net shaping of nickel-based superalloy inconel 718 powders onto aisi 4140 alloy steel substrates: Interface bond and fracture failure mechanism. Materials (Basel). 2017; 10.
85. C Huang, X Lin, F Liu, H Yang, W Huang. High strength and ductility of 34CrNiMo6 steel produced by laser solid forming. J. Mater. Sci. Technol. 2019; 35: 377–387.
86. Y Kakinuma, M Mori, Y Oda, T Mori, M Kashihara, et al. Influence of metal powder characteristics on product quality with directed energy deposition of Inconel 625. CIRP Ann. - Manuf. Technol. 2016; 65: 209–212.
87. A Ramakrishnan, GP Dinda. Direct laser metal deposition of Inconel 738. Mater. Sci. Eng. A. 2019; 740–741: 1–13.
88. H Xiao, S Li, X Han, J Mazumder, L Song. Laves phase control of Inconel 718 alloy using quasi-continuous-wave laser additive manufacturing. Mater. Des. 2017; 122: 330–339.
89. H Xiao, SM Lia, WJ Xiao, YQ Lia, LM Cha, et al. Effects of laser modes on Nb segregation and Laves phase formation during laser additive manufacturing of nickel-based superalloy. Mater. Lett. 2017; 188: 260–262.
90. G Singh, H Vasudev, A Bansal, S Vardhan, S Sharma. Microwave cladding of Inconel-625 on mild steel substrate for corrosion protection. Mater. Res. Express. 2020; 7.
91. VA Popovich, EV Borisov, AA Popovich, VS Sufiiarov, DV Masaylo, et al. Functionally graded Inconel 718 processed by additive manufacturing: Crystallographic texture,

anisotropy of microstructure and mechanical properties. Mater. Des. 2017; 114: 441–449.
92. H Xie, K Yang, F Li, C Sun, Z Yu. Investigation on the Laves phase formation during laser cladding of IN718 alloy by CA-FE. J. Manuf. Process. 2020; 52: 132–144.
93. K Yang, H Xie, C Sun, X Zhao, F Li. Influence of vanadium on the microstructure of IN718 alloy by laser cladding. Materials (Basel). 2019; 12: 1–12.
94. A Yadollahi, N Shamsaei, SM Thompson, DW Seely. Effects of process time interval and heat treatment on the mechanical and microstructural properties of direct laser deposited 316L stainless steel. Mater. Sci. Eng. A. 2015; 644: 171–183.
95. C Tan, K Zhou, T Kuang. Selective laser melting of tungsten-copper functionally graded material. Mater. Lett. 2019; 237: 328–331.
96. EO Olakanmi, M Sepako, J Morake, SE Hoosain, SL Pityana. Microstructural Characteristics, Crack Frequency and Diffusion Kinetics of Functionally Graded Ti-Al Composite Coatings: Effects of Laser Energy Density (LED). Jom. 2019; 71: 900–911.
97. G Bidron, A Doghri, T Malot, F Fournier-dit-Chabert, M Thomas, et al. Reduction of the hot cracking sensitivity of CM-247LC superalloy processed by laser cladding using induction preheating. J. Mater. Process. Technol. 2020; 277: 116461.
98. U Savitha, G Jagan Reddy, A Venkataramana, A Sambasiva Rao, AA Gokhale, et al. Chemical analysis, structure and mechanical properties of discrete and compositionally graded SS316-IN625 dual materials. Mater. Sci. Eng. A. 2015; 647: 344–352.
99. RM Mahamood, ET Akinlabi. Laser metal deposition of functionally graded Ti6Al4V/TiC. Mater. Des. 2015; 84: 402–410.
100. L Li, J Wang, P Lin, H Liu. Microstructure and mechanical properties of functionally graded TiCp/Ti6Al4V composite fabricated by laser melting deposition. Ceram. Int. 2017; 43: 16638–16651.
101. J Zhang, Y Zhang, W Li, S Karnati, F Liou, et al. Microstructure and properties of functionally graded

materials Ti6Al4V/TiC fabricated by direct laser deposition. Rapid Prototyp. J. 2004; 10: 5–6.

102. LD Bobbio, RA Otis, JP Borgonia, RP Dillon, AA Shapiro, et al. Additive manufacturing of a functionally graded material from Ti-6Al-4V to Invar: Experimental characterization and thermodynamic calculations. Acta Mater. 2017; 127: 133–142.

103. SN Li, HP Xiong, N Li, BQ Chen, C Gao, et al. Mechanical properties and formation mechanism of Ti/SiC system gradient materials fabricated by in-situ reaction laser cladding. Ceram. Int. 2017; 43: 961–967.